Preprints of the 8th IFAC Symposium on Advanced Control of Chemical Processes
The International Federation of Automatic Control
Furama Riverfront, Singapore, July 10-13, 2012

Control structure design for stabilizing unstable gas-lift oil wells

Esmaeil Jahanshahi, Sigurd Skogestad [1] and Henrik Hansen

Department of Chemical Engineering, Norwegian University of Science and technology, Trondheim, NO-7491 (e-mail: skoge@ntnu.no).

Abstract: Active control of the production choke valve is the recommended solution to prevent casing-heading instability in gas-lifted oil wells. Focus of this work is to find a simple yet robust control structure for stabilization of the system. In order to find suitable control variables, a controllability analysis of the system with different candidate control variables and two alternative manipulated variables was performed. Moreover, to include robustness and performance requirements at the same time, the controllability analysis was extended to a mixed sensitivity $\mathcal{H}_\infty$ optimization problem. A control structure using only the available top-side pressure measurements was found to be effective to stabilize this system.

Keywords: Oil production, two-phase flow, gas-lift, controllability, $\mathcal{H}_\infty$ control.

1. INTRODUCTION

Gas-lift is one of the processes which are used to artificially lift oil from wells where there is insufficient reservoir pressure to produce from the well. This method is also used for increasing the production rate of oil wells. In this process, gas is routed from the surface into the annulus and then injected deep into the tubing in order to be mixed with the fluid from the reservoir. This reduces the density of the column of fluid in the tubing and lightens it, Leads to a lower pressure at the bottom-hole. Hence the production rate from the low pressure reservoir is increased.

Gas-lifted oil wells often become unstable at their decline stages. The unstable operation is characterized by large oscillatory variations in the pressure and the production rate. There are several phenomena causing instability in gas-lifted oil wells; we focus on the "casing-heading" instability in this paper.

The oscillatory flow condition is undesirable and an effective solution is needed to prevent it. The conventional solutions include reducing the opening of the production choke valve and increasing the amount of the injected gas. However, closing the production choke increases the back pressure of the valve, and reduces the production rate from the oil well; also increasing the injected gas is costly.

Automatic control was first used by Jansen et al. (1999) to stabilize unstable gas-lifted oil wells. Measurements such as pressure, flow rate or fluid density are used as the control variables and the top-side choke valves are the manipulated variables. The bottom-hole pressure in well is the recommended control variable for anti-slug control of gas-lift wells, but this measurement is not available usually. Therefore, Eikrem et al. (2004) and Aamo et al. (2005) utilized model-based observers to estimate bottom-hole pressure from top-side measurements.

We look for other possibilities for anti-slug control of gas-lift oil wells. In this way, we examine all of possible measured variables of the system to find suitable control variables for stabilization. In addition, we consider the gas-lift choke valve as a secondary manipulated variable and we examine if using the second manipulated variable improves the control. Similar works on control structure design for stabilizing riser slugging has been done by Sivertsen et al. (2009), Storkaas and Skogestad (2007).

The controllability analysis is used as a tool to find control variables satisfying performance and robustness requirements. The controllability is evaluated by minimum achievable peaks of different closed-loop transfer functions. The control variables or combinations of them resulting in smaller peaks are preferred (Skogestad and Postlethwaite (2005)).

However, the controllability analysis is a mathematical tool for linear systems. Knowing that nature of the system and even the simplified model used in this work is highly nonlinear, the controllability analysis only gives insight into the necessary conditions and limitations.

For the controllability analysis and the model-based control design, a simple dynamical model of the system is preferred. First, a three-state model for casing-heading instability was developed in ABB AS, then Dvergsnes (1999) added two states for energy in annulus and tubing. Imsland (2002) ignored the two energy states, but he used more sophisticated pressure drop calculations. A simplified version of the Imsland model was used by Eikrem et al. (2004) which is the basis of the model presented in this paper. We add a pressure loss term due to friction, also we use a new approach by Jahanshahi and Skogestad (2011) for calculating phase fractions and density at top of the tubing.

This paper is organized as the following. A modified simplified model for the casing heading instability is introduced in Section 2. Afterwards, the theoretical background for the controllability analysis is given in Section 3, then controllability analysis results are presented in Section 4. In section 5, we choose suitable control structures, and finally the main conclusions and remarks will be summarized in Section 6.

[1] Corresponding author

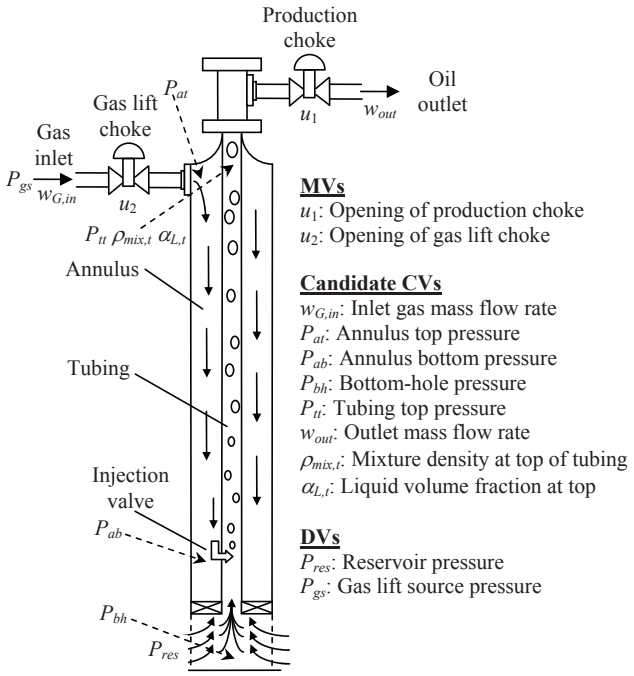

Fig. 1. Schematic presentation of candidate control variables and manipulated variables

2. SIMPLIFIED DYNAMICAL MODEL

A schematic illustration of gas-lift oil wells is shown in Fig. 1. Similar to the model introduced by Eikrem et al. (2004), state variables of our model are x_1 mass of gas in the annulus, x_2 mass of gas in the tubing and x_3 mass of liquid in the tubing. We consider also production of gas from the reservoir, therefore our state equations are in the following form:

$$\dot{x}_1 = w_{G,in} - w_{G,inj} \tag{1}$$

$$\dot{x}_2 = w_{G,inj} + w_{G,res} - w_{G,out} \tag{2}$$

$$\dot{x}_3 = w_{L,res} - w_{L,out} \tag{3}$$

In this model, $w_{G,in}$ is the mass flow rate of inlet gas to the annulus and $w_{G,inj}$ is the mass flow of injected gas from the annulus into the tubing. $w_{G,res}$ and $w_{L,res}$ are gas and liquid mass flow rates from the reservoir to the tubing. $w_{G,out}$ and $w_{L,out}$ are the mass flow rates of gas and oil outlet from the tubing, respectively.
There is only gas phase inside the annulus, and pressure at top of the annulus can be calculated by ideal gas law.

$$P_{at} = \frac{RT_a x_1}{M_G V_a} \tag{4}$$

Then, the pressure at bottom of the annulus is given by

$$P_{ab} = P_{at} + \frac{x_1 g L_a}{V_a}, \tag{5}$$

Thus, the density of the gas phase at this point is

$$\rho_{G,ab} = \frac{P_{ab} M_G}{RT_a}. \tag{6}$$

The inlet gas to the annulus comes from a source tank or a compressor with the pressure P_{gs}, and the density of gas through the gas-lift choke can be written as:

$$\rho_{G,in} = \frac{P_{gs} M_G}{RT_a} \tag{7}$$

Therefore, gas mass flow into the annulus is

$$w_{G,in} = K_{gs} u_2 \sqrt{\rho_{G,in} max(P_{gs} - P_{at}, 0)}. \tag{8}$$

Because of high pressure, the fluid from the reservoir is saturated (Ahmed (2006)). Hence, we assume that distance between the bottom-hole and the injection point, L_{bh}, is filled by liquid phase. This must be accounted for in calculating the volume of gas in the tubing. Consequently, the density of gas at top of the tubing follows as

$$\rho_{G,t} = \frac{x_2}{V_t + S_{bh} L_{bh} - x_3/\rho_L}. \tag{9}$$

Pressure at top of tubing using ideal gas law:

$$P_{tt} = \frac{\rho_{G,t} RT_t}{M_G} \tag{10}$$

Average mixture density inside tubing:

$$\overline{\rho}_{mix} = \frac{x_2 + x_3 - \rho_L S_{bh} L_{bh}}{V_t} \tag{11}$$

Average liquid volume fraction inside tubing:

$$\overline{\alpha}_L = \frac{x_3 - \rho_L S_{bh} L_{bh}}{V_t \rho_L} \tag{12}$$

GOR is the constant mass ratio of gas and liquid produced from the reservoir, and gas mass fraction at bottom of the tubing is

$$\alpha^m_{G,b} = GOR/(GOR + 1). \tag{13}$$

Before calculating the inlet mass flow rate from the reservoir by use of the bottom-hole pressure in equation (27), the pressure drop due to friction is needed to determine the bottom-hole pressure. However, we need to know the inlet flow rate to calculate the friction term. We evade this problem by using an average of the inlet flow rate, $\overline{w}_{res}$, in calculation of friction terms.
Average superficial velocity of liquid phase in tubing:

$$\overline{U}_{sl,t} = \frac{4(1 - \alpha^m_{G,b})\overline{w}_{res}}{\rho_L \pi D_t^2} \tag{14}$$

Average superficial velocity of gas phase:

$$\overline{U}_{sg,t} = \frac{4(w_{G,in} + \alpha^m_{G,b}\overline{w}_{res})}{\rho_{G,t} \pi D_t^2} \tag{15}$$

We have not calculated flow rate of the injected gas from the annulus into the tubing yet, instead we use $w_{G,in}$ in equation (15); we believe averages of these two variables are equal.
Average mixture velocity in tubing:

$$\overline{U}_{m,t} = \overline{U}_{sl,t} + \overline{U}_{sg,t} \tag{16}$$

Reynolds number of flow in tubing:

$$Re_t = \frac{\overline{\rho}_{mix} \overline{U}_{m,t} D_t}{\mu} \tag{17}$$

An explicit approximation of the implicit Colebrook-White equation proposed by Haaland (1983) is used as the friction factor in the tubing.

$$\frac{1}{\sqrt{\lambda_t}} = -1.8\log_{10}\left[\left(\frac{\epsilon/D_t}{3.7}\right)^{1.11} + \frac{6.9}{Re_t}\right] \tag{18}$$

Pressure loss due to friction in tubing:

$$F_t = \frac{\overline{\alpha}_L \lambda_t \overline{\rho}_{mix} \overline{U}_{m,t}^2 L_t}{2D_t} \tag{19}$$

Pressure at bottom of the tubing where gas being injected from annulus:

$$P_{tb} = P_{tt} + \overline{\rho}_{mix} g L_t + F_t \tag{20}$$

Mass flow rate of gas injected into tubing:

$$w_{G,inj} = K_{inj}\sqrt{\rho_{G,ab} max(P_{ab} - P_{tb}, 0)} \tag{21}$$

Liquid velocity at bottom-hole:

$$\overline{U}_{l,b} = \frac{\overline{w}_{res}}{\rho_L S_{bh}} \tag{22}$$

Reynolds number of flow at bottom-hole:

$$Re_b = \frac{\rho_L \overline{U}_{l,b} D_b}{\mu} \tag{23}$$

Friction factor at bottom-hole:

$$\frac{1}{\sqrt{\lambda_b}} = -1.8\log_{10}\left[\left(\frac{\epsilon/D_b}{3.7}\right)^{1.11} + \frac{6.9}{Re_b}\right] \tag{24}$$

Pressure loss due to friction from bottom-hole to injection point:

$$F_b = \frac{\lambda_b \rho_L \overline{U}_{l,b}^2 L_{bh}}{2D_b} \tag{25}$$

Pressure at bottom-hole:

$$P_{bh} = P_{tb} + F_b + \rho_L g L_{bh} \tag{26}$$

Mass flow rate from reservoir to tubing:

$$w_{res} = PI max(P_{res} - P_{bh}, 0) \tag{27}$$

Mass flow rate of liquid from reservoir to tubing:

$$w_{L,res} = (1 - \alpha_{G,b}^m) w_{res} \tag{28}$$

Mass flow rate of gas from reservoir to the well:

$$w_{G,res} = \alpha_{G,b}^m w_{res} \tag{29}$$

Density of gas at bottom of tubing:

$$\rho_{G,tb} = \frac{P_{tb} M_G}{R T_t} \tag{30}$$

Liquid volume fraction at bottom of tubing:

$$\alpha_{L,b} = \frac{w_{L,res}\rho_{G,tb}}{w_{L,res}\rho_{G,tb} + (w_{G,inj} + w_{G,res})\rho_L} \tag{31}$$

With the same assumptions used by Jahanshahi and Skogestad (2011), liquid volume fraction at top of the tubing can be written as

$$\alpha_{L,t} = 2\overline{\alpha}_L - \alpha_{L,b}, \tag{32}$$

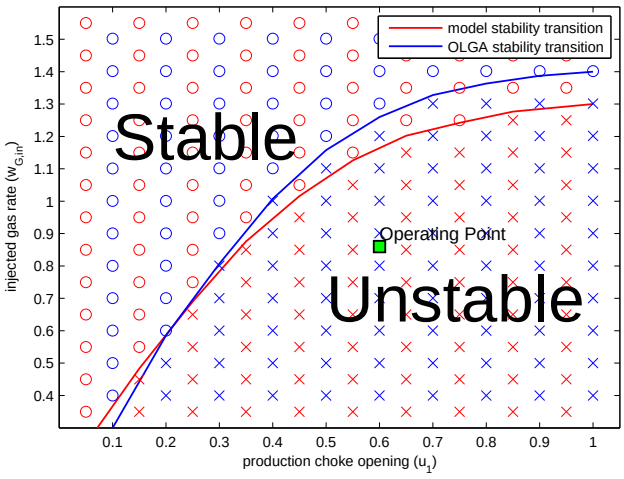

Fig. 2. Stability transition of system, blue markers for OLGA and red markers for simplified model

Then, the mixture density at top of the tubing will be

$$\rho_{mix,t} = \alpha_{L,t}\rho_L + (1 - \alpha_{L,t})\rho_{G,t}. \tag{33}$$

Mass flow rate of mixture from production choke:

$$w_{out} = K_{pr} u_1 \sqrt{\rho_{mix,t} max(P_{tt} - P_0, 0)} \tag{34}$$

Volumetric flow rate of production choke:

$$Q_{out} = w_{out}/\rho_{mix,t} \tag{35}$$

Gas mass fraction at top of tubing:

$$\alpha_{G,t}^m = \frac{(1 - \alpha_{L,t})\rho_{G,t}}{\alpha_{L,t}\rho_L + (1 - \alpha_{L,t})\rho_{G,t}} \tag{36}$$

Mass flow rate of outlet gas from tubing:

$$w_{G,out} = \alpha_{G,t}^m w_{out} \tag{37}$$

Mass flow rate of outlet liquid from tubing:

$$w_{L,out} = (1 - \alpha_{G,t}^m) w_{out} \tag{38}$$

The simplified model was fitted to a test case implemented in the OLGA simulator. Constants and parameters used in the model are given in Table 1. The stability map of the system is shown in Fig. 2 where stability transitions of the OLGA model and the simplified model are compared. The controllability analysis and all simulations are performed at the operating point $u_1 = 0.6$ and $w_{G,in} = 0.86$ $[kg/s]$ which is located in the unstable region of the stability map. It was not possible to add the gas-lift choke to the OLGA model, therefore we used a constant gas source equal to $w_{G,in} = 0.8$ $[kg/s]$ in the OLGA model and we fitted the model with the constant gas rate. Then, we added the gas-lift choke valve to the Matlab model so that the simplified model gives $w_{G,in} = 0.8$ $[kg/s]$ when the gas-lift choke opening is $u_2 = 0.4$ and the production choke opening is $u_1 = 0.3$. The system switches from stable to unstable at this operating point. Finally, we opened the production valve to $u_1 = 0.6$ in order to make the system unstable; the inlet gas rate becomes $w_{G,in} = 0.86$ $[kg/s]$ at this operating point.

3. CONTROLLABILITY ANALYSIS: THEORETICAL BACKGROUND

The state controllability is not considered in this work; instead the concept of input-output controllability as defined by Skogestad and Postlethwaite (2005) is used.

Definition 1. **(Input-output) controllability** *is the ability to achieve acceptable control performance; that is, to keep the outputs (y) within specified bounds or displacements from their references (r), in spite of unknown but bounded variations, such as disturbances (d) and plant changes (including uncertainty), using available inputs (u) and available measurements (y_m and d_m).*

The ability of the system to reach performance and robustness requirements with the control can be evaluated quantitatively by calculating minimum achievable peaks of different closed-loop transfer functions. These peaks are related to physical limitations of a the system in terms of controllability and they are dependent on the location of poles and zeros of the open-loop system.

3.1 Transfer functions

We assume a linear model in the form $y = G(s)u + G_d(s)d$ with a feedback controller $u = K(s)(r - y - n)$ in which d represents disturbances and n is the measurement noise. The resulting closed-loop system is

$$y = Tr + SG_d d - Tn, \tag{39}$$

where $S = (I + GK)^{-1}$ and $T = GK(I + GK)^{-1} = I - S$ represent the sensitivity and the complementary sensitivity transfer functions, respectively. The control input to the closed-loop system is

$$u = KS(r - G_d d - n). \tag{40}$$

In addition to the transfer functions introduced above, the transfer function SG is related to the effect of input disturbances on the control error $r - y$. The closed-loop transfer functions S, T, KS and SG can also be regarded as the measures of robustness against different types of uncertainty. We prefer to keep them as small as possible to achieve better robustness properties of the control system. For instance, the sensitivity transfer function S is also the sensitivity to inverse relative uncertainty, which is a good indication of uncertainty in the pole locations (Skogestad and Postlethwaite (2005)). Therefore, the lowest achievable peaks of the closed-loop transfer functions S, T, KS, SG, KSG_d and SG_d provide information regarding both achievable performance and possible robustness issues.

Table 1. Parameters values used in simulations

Symb.	Description	Values	Units
R	universal gas constant	8314	$J/(kmol.K)$
g	gravity	9.81	m/s^2
μ	viscosity	3.64×10^{-3}	$Pa.s$
ρ_L	liquid density	760	kg/m^3
M_G	gas molecular weight	16.7	gr
T_a	annulus temperature	348	K
V_a	annulus volume	64.34	m^3
L_a	annulus length	2048	m^3
P_{gs}	gas source pressure	140	bar
V_t	tubing volume	25.03	m^3
S_{bh}	cross-section below injection point	0.0314	m^2
L_{bh}	length below injection point	75	m
T_t	tubing temperature	369.4	K
GOR	mass gas oil ratio	0	–
P_{res}	reservoir pressure	160	bar
$\overline{w}_{res}$	average mass flow from reservoir	18	kg/s
D_t	tubing diameter	0.134	m
L_t	tubing length	2048	m
PI	productivity index	2.47e-6	$kg/(s.Pa)$
K_{gs}	gas-lift choke cons.	9.98×10^{-5}	–
K_{inj}	injection valve cons.	1.40×10^{-4}	–
K_{pr}	production choke cons.	2.90×10^{-3}	–

By the "peak" we mean maximum value of frequency response or $\mathcal{H}_\infty$ norm, $\|M\|_\infty = \max_\omega \|M(j\omega)\|$, that is simply the peak value of the transfer function. The bounds are not dependent on the controller K, and they are physical properties of the system itself. The bounds are, however, dependent on a systematic and correct scaling of the system. Scaling of the system will be explained later in this Section.

The lowest achievable peaks in sensitivity and complementary sensitivity transfer functions, denoted $M_{S,min}$ and $M_{T,min}$, are closely related to the distance between the unstable poles (p_i) and zeros (z_i). Considering SISO systems, for any unstable (RHP) zero z:

$$\|S\|_\infty \geq M_{S,min} = \prod_{i=1}^{N_p} \frac{|z + p_i|}{|z - p_i|}. \tag{41}$$

Note that the bound approaches infinity as z approaches p_i. For systems with only one unstable zero, the bound holds with equality.

Formulae for calculating bounds on minimum achievable peaks of the other closed-loop transfer functions are given by Skogestad and Postlethwaite (2005), also by Storkaas and Skogestad (2007).

3.2 Mixed Sensitivity Controllability Analysis

The above controllability measures were also considered by Sivertsen et al. (2009), Storkaas and Skogestad (2007). However, these measures considering only one of transfer functions at any time, may give conflicting results. To get a single measure (γ), we consider an $\mathcal{H}_\infty$ problem where we want to bound $\overline{\sigma}(S)$ for performance, $\overline{\sigma}(T)$ for robustness and to avoid sensitivity to noise and $\overline{\sigma}(KS)$ to penalize large inputs. These requirements may be combined into a stacked $\mathcal{H}_\infty$ problem (Skogestad and Postlethwaite (2005)).

$$\min_K \|N(K)\|_\infty, \quad N \triangleq \begin{bmatrix} W_u KS \\ W_T T \\ W_P S \end{bmatrix} \tag{42}$$

where W_P and W_T determine the desired shapes of sensitivity S and complementary sensitivity T. Typically, W_P^{-1} is chosen to be small at low frequencies to achieve good disturbance attenuation (i.e., performance), and W_T^{-1} is chosen to be small outside the control bandwidth, which helps to ensure good stability margin (i.e., robustness). Solution to this optimization problem is a stabilizing controller K corresponding to S, T and KS which satisfy the following loop shaping inequalities:

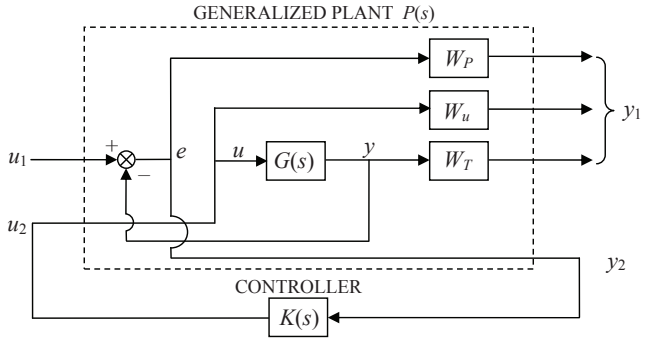

Fig. 3. Closed-loop transfer function for mixed sensitivity control design

$$\begin{aligned} \overline{\sigma}(KS(j\omega)) &\leq \gamma \underline{\sigma}(W_u^{-1}(j\omega)) \\ \overline{\sigma}(T(j\omega)) &\leq \gamma \underline{\sigma}(W_T^{-1}(j\omega)) \\ \overline{\sigma}(S(j\omega)) &\leq \gamma \underline{\sigma}(W_P^{-1}(j\omega)) \end{aligned} \tag{43}$$

To have the same cost function in all simulation tests for the measurement selection, all the candidate control variables shown in Fig. 1 are included in the y_1 port and the control variable(s) for test is in the port y_2 of the generalized plant in Fig. 3. The value of γ in equation (43) should be as small as possible for good controllability.

3.3 Scaling

One important step before controllability analysis is scaling of inputs, outputs and disturbances of the model. In *Definition 1*, the bound that the control variable must be kept within is not the same for different control variables shown in Fig. 1. For a correct comparison between candidate control variables, they must be scaled based on their maximum allowed variations, in a way that maximum allowed variation for all of them in the scaled model become (-1,1). The scaling factors D_y for different measurements are given in Table 2. Disturbances in the scaled model are also expected to vary in the range of $(-1, 1)$. The maximum expected value of the both disturbances (P_{res} and P_{gs}) is 3 *bar* variation around their nominal values. Therefore, the scaling matrix of the disturbances:

$$D_d = \begin{bmatrix} 3 & 0 \\ 0 & 3 \end{bmatrix}.$$

Controllability analysis is performed at the operating point $u_1 = 0.6$ and $u_2 = 0.4$. Valves can go to filly-open or fully-closed condition, therefore the maximum possible change for the both manipulated variables is 0.4, this means

$$D_u = \begin{bmatrix} 0.4 & 0 \\ 0 & 0.4 \end{bmatrix}.$$

4. CONTROLLABILITY ANALYSIS RESULTS

4.1 Bounds on Minimum Achievable Peaks

Minimum achievable peaks for different closed-loop transfer functions are given in Table 2 and Table 3. Minimum peaks of $|S| = |T|$ for P_{tt}, $\rho_{mix,t}$ and $\alpha_{L,t}$ in Table 2 are larger than 1, and it is expected to have difficulty using these measurements as control variables.
The reason for large values of $|S| = |T|$ is RHP-zeros in

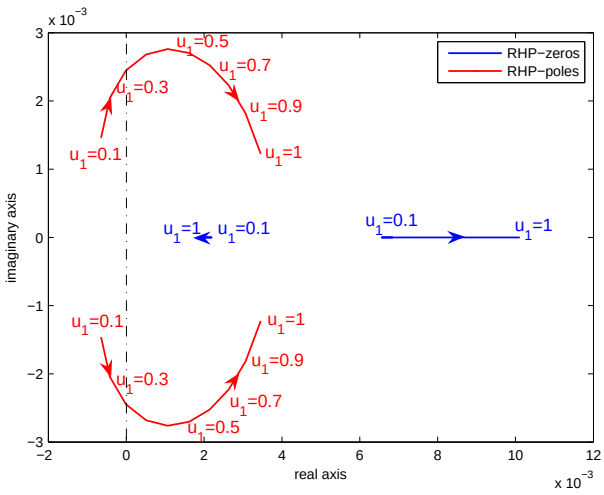

Fig. 4. Location of RHP-poles of system and RHP-zeros of tubing top pressure for $u_2 = 0.4$ and different values of u_1

transfer functions. Location of RHP-poles of the system and RHP-zeros of P_{tt} for $u_2 = 0.4$ and different production choke openings u_1 are shown in Fig. 4. The system has a pair of complex conjugate poles on the imaginary axis for $u_1 = 0.3$. These two poles move to the RHP and the system becomes unstable for $u_1 > 0.3$; this is in agreement with the stability map in Fig. 2. P_{tt} shows two RHP-zeros for all u_1 values. One of the RHP-zeros does not move so much and it is always close to pole locations. As the production valve opening u_1 increases, RHP-poles get closer to the smaller (important) RHP-zero. According to equation (41), the closer poles and zeros are, the larger the peak of sensitivity transfer function becomes.
The pressure at top of the tubing, P_{tt}, is not recommended to be used as a single control variable, but the large peak of sensitivity does not occur when it combines with other measurement. The minimum achievable peak of sensitivity transfer function for the paired measurements becomes 1 in Table 2, because the system becomes non-square and zeros disappear.
The bottom-hole pressure P_{bh} shows the best controllability properties. It has the largest element in the output pole vector that makes it suitable for stabilization of the unstable system. Moreover, P_{bh} has the largest steady-state gain $G(0)$ and the smallest values for all of the closed-loop transfer functions. In the second place, the pressure at the bottom of the annulus shows good controllability properties. The third good candidate is the pressure at top of the annulus, P_{at}.

4.2 Mixed Sensitivity Controllability Analysis

The γ values are given in Table 2 and Table 3. Control structures with small value of γ are able to reach performance, robustness and input requirements easier. The bottom-hole pressure shows the smallest γ among the single measurements; it is consistent with the other controllability data. Moreover, combination of the bottom-hole pressure and the tubing top pressure results in the smallest γ for the both single manipulated variable and the related MIMO case.
Using two control variables and one manipulated variable,

Table 2. Controllability data using u_1 as manipulated variable

Measurement	Value	D_y	$G(0)$	Pole vector	$\|S\| = \|T\|$	$\|KS\|$	$\|SG\|$	$\|KSG_{d1}\|$	$\|KSG_{d2}\|$	$\|SG_{d1}\|$	$\|SG_{d2}\|$	γ_1	γ_2
$w_{gin}[kg/s]$	0.86	0.05	0.76	0.0004	1.00	3.04	0.00	0.23	1.987	0.00	0.00	89.55	–
$P_{at}[bar]$	81.16	1	5.22	0.0031	1.00	0.44	0.00	0.23	0.10	0.00	0.00	14.85	–
$P_{tt}[bar]$	20.89	1	5.72	0.0028	3.06	0.38	10.49	0.25	0.11	0.69	0.42	19.16	–
$P_{ab}[bar]$	90.35	1	5.81	0.0034	1.00	0.40	0.00	0.23	0.10	0.00	0.00	13.54	–
$P_{bh}[bar]$	88.56	1	6.95	0.0089	1.00	0.11	0.00	0.23	0.09	0.00	0.00	3.60	–
$w_{out}[kg/s]$	18.51	2	0.88	0.0024	1.00	0.49	0.00	0.30	0.11	0.00	0.00	19.35	–
$\rho_{mix,t}[kg/m^3]$	186.96	20	1.61	0.0013	3.11	1.24	3.77	0.56	0.29	0.71	0.38	38.08	–
$\alpha_{L,t}[-]$	0.23	0.23	0.17	0.0001	3.11	10.83	0.43	0.57	0.30	0.08	0.04	289.88	–
P_{ab} w_{out}	–	–	–	0.0034	1.00	0.26	0.00	0.13	0.05	0.00	0.00	8.89	19.35
P_{ab} ρ_{mix}	–	–	–	0.0034	1.00	0.36	0.00	0.20	0.08	0.00	0.00	12.20	13.17
P_{ab} $w_{G,in}$	–	–	–	0.0034	1.00	0.40	0.00	0.12	0.10	0.00	0.00	13.42	22.13
P_{at} P_{bh}	–	–	–	0.0089	1.00	0.11	0.00	0.12	0.05	0.00	0.00	4.52	3.45
P_{at} P_{tt}	–	–	–	0.0031	1.00	0.26	0.00	0.12	0.05	0.00	0.00	8.65	11.58
P_{at} w_{out}	–	–	–	0.0031	1.00	0.27	0.00	0.13	0.05	0.00	0.00	9.17	19.35
P_{at} ρ_{mix}	–	–	–	0.0031	1.00	0.39	0.00	0.20	0.08	0.00	0.00	13.12	13.96
P_{at} $w_{G,in}$	–	–	–	0.0031	1.00	0.44	0.00	0.12	0.10	0.00	0.00	14.70	22.13
P_{bh} w_{out}	–	–	–	0.0089	1.00	0.10	0.00	0.13	0.05	0.00	0.00	3.39	19.35
P_{bh} ρ_{mix}	–	–	–	0.0089	1.00	0.11	0.00	0.20	0.09	0.00	0.00	3.53	10.96
P_{bh} $w_{G,in}$	–	–	–	0.0089	1.00	0.11	0.00	0.12	0.10	0.00	0.00	3.60	22.13
P_{tt} P_{bh}	–	–	–	0.0089	1.00	0.10	0.00	0.12	0.05	0.00	0.00	7.25	3.39
P_{tt} w_{out}	–	–	–	0.0028	1.00	0.30	0.00	0.14	0.06	0.00	0.00	15.41	19.35
P_{tt} ρ_{mix}	–	–	–	0.0028	1.00	0.34	0.00	0.21	0.10	0.00	0.00	16.97	12.23
P_{tt} $w_{G,in}$	–	–	–	0.0028	1.00	0.37	0.00	0.12	0.12	0.00	0.00	18.64	22.13
w_{out} $w_{G,in}$	–	–	–	0.0024	1.00	0.47	0.00	0.13	0.12	0.00	0.00	19.35	22.13

Table 3. Controllability data using u_1 and u_2 as manipulated variables (MIMO controller)

Measurement	Pole vector	$\|S\| = \|T\|$	$\|KS\|$	$\|SG\|$	$\|KSG_{d1}\|$	$\|KSG_{d2}\|$	$\|SG_{d1}\|$	$\|SG_{d2}\|$	γ_1	γ_2	γ_3
P_{ab} w_{out}	0.0034	1.00	0.12	0.00	0.08	0.03	0.00	0.00	7.55	13.20	15.31
P_{ab} $\rho_{mix,t}$	0.0034	1.50	0.14	2.00	0.11	0.05	0.34	0.12	10.39	12.16	16.53
P_{ab} $w_{G,in}$	0.0034	1.00	0.16	0.00	0.09	0.07	0.00	0.00	11.43	10.98	12.40
P_{at} P_{bh}	0.0089	1.00	0.07	0.00	0.08	0.03	0.00	0.00	3.94	3.20	14.47
P_{at} P_{tt}	0.0031	1.59	0.13	11.00	0.08	0.03	0.96	0.62	7.36	7.76	8.16
P_{at} w_{out}	0.0031	1.00	0.13	0.00	0.08	0.03	0.00	0.00	7.83	12.30	15.33
P_{at} $\rho_{mix,t}$	0.0031	1.52	0.15	1.87	0.11	0.05	0.32	0.11	11.23	12.89	16.74
P_{at} $w_{G,in}$	0.0031	1.00	0.18	0.00	0.09	0.07	0.00	0.00	12.59	12.20	13.63
P_{bh} w_{out}	0.0089	1.00	0.07	0.00	0.08	0.04	0.00	0.00	3.15	13.30	75.80
P_{bh} $\rho_{mix,t}$	0.0089	1.02	0.07	7.71	0.11	0.06	1.05	0.52	3.28	10.07	32.09
P_{bh} $w_{G,in}$	0.0089	1.00	0.07	0.00	0.09	0.09	0.00	0.00	3.35	3.20	3.58
P_{tt} P_{bh}	0.0089	1.20	0.07	16.73	0.08	0.04	1.04	0.64	5.19	3.15	5.22
P_{tt} w_{out}	0.0028	2.05	0.19	0.00	0.09	0.04	1.04	0.64	11.37	13.30	12.33
P_{tt} $\rho_{mix,t}$	0.0028	2.15	0.20	19.48	0.12	0.06	1.69	0.95	12.18	11.35	13.09
P_{tt} $w_{G,in}$	0.0028	2.69	0.25	19.38	0.09	0.09	1.14	1.09	14.15	8.78	16.56
w_{out} $w_{G,in}$	0.0024	1.00	0.30	0.00	0.10	0.09	0.00	0.00	13.30	11.32	21.55

it is impossible to get tight control on the both control variables at the same time. Similar to a cascade controller, we can have tight control with a constant set-point only on one of control variables.

In Table 2, we calculated γ_1 when tight control was required on the first control variable of the pair, and γ_2 when tight control was on the second one in the pair.

Uisng two manipulated variables, it was possible to have tight control on the both control variables in the pairs; γ_3 values in Table 3 were calculated for this condition. γ_1 and γ_2 in Table 3 can be compared to those in Table 2, but the cost function related to the $\mathcal{H}_\infty$ problem for calculating the γ_3 values is different.

5. CONTROL STRUCTURE SELECTION

Based on the controllability data provided in Table 2 and Table 3, we can decide about choosing the control structure. For a SISO control structure, pressure at bottomhole P_{bh} is the best control variables in our results. It is in accordance with previous works in which always P_{bh} has been favored. P_{bh} usually is not directly measurable, but as suggested by Eikrem et al. (2004) and Aamo et al. (2005), it can estimated using an observer. Simulation result of using this measurement is shown in Fig 5. Simulation results of using P_{tt} and P_{at} are shown in Fig 6 and Fig 7, respectively. The both P_{tt} and P_{at} demonstrate poor performance when they are used for SISO control. All of the simulations are based on scaled variables, and the ideal is to keep the control variables in the range of (-1,1).

Looking at paired control variables with u_1 as the manipulated variable in Table 2, all parings including P_{bh} with tight control on P_{bh} result in small γ values. However, there is no significant improvement in γ values compared to using the single control variable P_{bh}; simulation result of combing P_{bh} and w_{out} is shown in Fig. 8. The next suitable combination is the pair of P_{at} and P_{tt} (two topside pressures) with tight control on P_{at}. The simulation result for this case is given in Fig. 9.

We did controllability analysis also by using u_2 as the

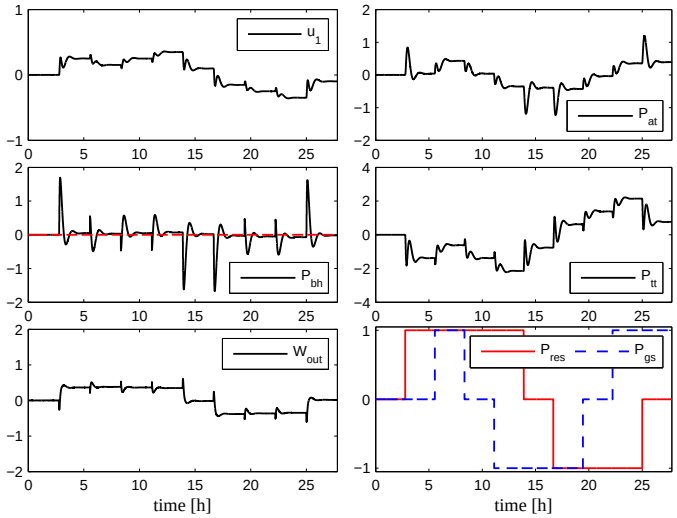

Fig. 5. Simulation result of $\mathcal{H}_\infty$ control using P_{bh} as control variable and u_1 as manipulated variable

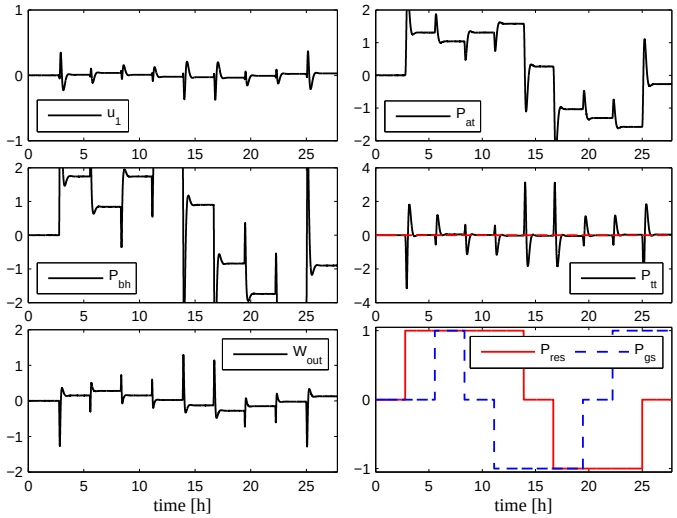

Fig. 6. Simulation result of $\mathcal{H}_\infty$ control using P_{tt} as control variable and u_1 as manipulated variable

single manipulating variable, but the results using u_2 were not satisfactory and we did not add another large table for sake of the space limitation. The simulation result using relatively the best pair of control variables for this case, resulted in $\gamma_2 = 14.1$, is shown in Fig. 10.

Looking at Table 3, the pairs with P_{bh} show small γ values, but compared to the γ values in Table 2, there is no substantial improvement. The simulation result of using the two top-side pressure measurement, P_{at} and P_{tt}, using two manipulated variables is shown in Fig. 11.

The pressures at top can be easily measured with good accuracy and a control structure using their combination (Fig. 9) is recommended. However, by comparing simulation results in Fig. 9 and Fig. 11, one should notice that adding the secondary manipulated variable does not enhance the control performance.

The choice of the suitable control structure is dependant on proper scaling of the control variables. For example for this case, first we chose a small scaling factor for the mass flow rate and we wanted to control it in a tight bound.

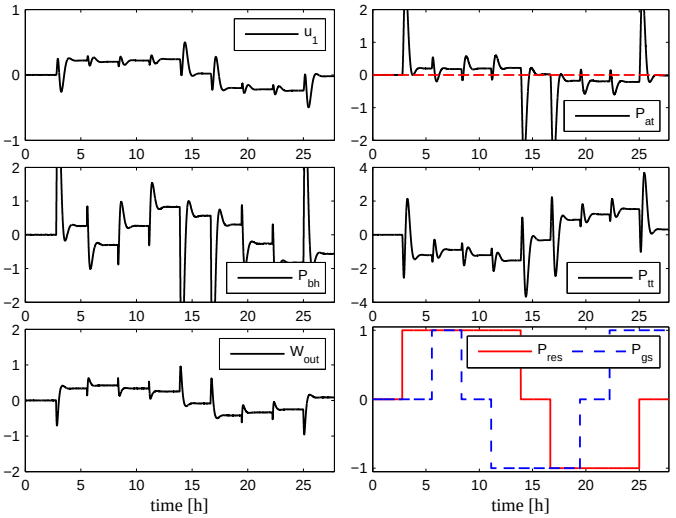

Fig. 7. Simulation result of $\mathcal{H}_\infty$ control using P_{at} as control variables and u_1 as manipulated variable

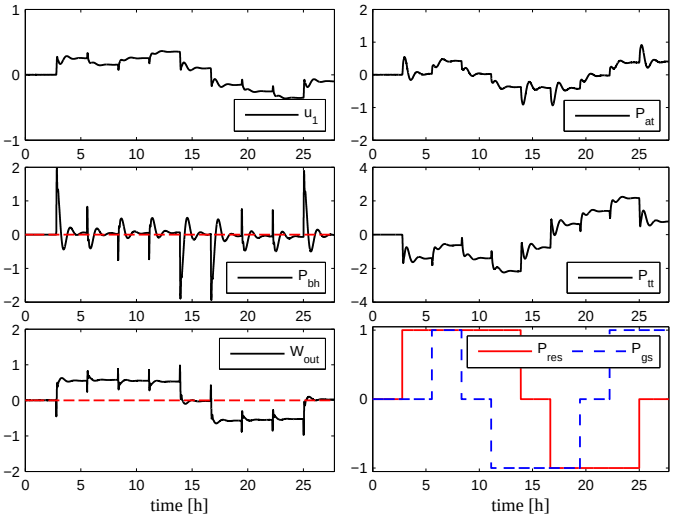

Fig. 8. Simulation result of $\mathcal{H}_\infty$ control using P_{bh} and w_{out} as control variables and u_1 as manipulated variable

As a result, gain of the system with this control variable increased and the control structures using the flow rate resulted in better performance compared to those using the pressures. In order to control the flow rate in a tight range, we must be able to measure it accurately. However, this is unlikely for two-phase flow in practice. Therefore, we chose a wider scaling factor for the flow rate. On the other hand, pressure can be measured more reliably, thus a small scaling factor was used for pressures. Consequently, the control structures using pressure measurements are shown to be superior for this case study.

6. CONCLUSION

An improved dynamical model for the casing-heading instability in gas-lifted oil wells was proposed, then the proposed model was fitted to a rigorous model in the OLGA simulator. Minimum achievable peaks of the different closed-loop transfer functions with each of the candidate control variables and their combinations were calculated.

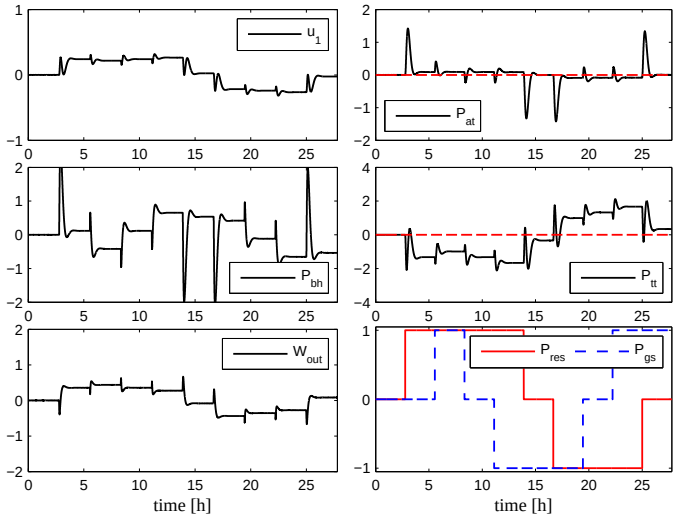

Fig. 9. Simulation result of $\mathcal{H}_\infty$ control for P_{at} and P_{tt} as control variables and u_1 as manipulated variable

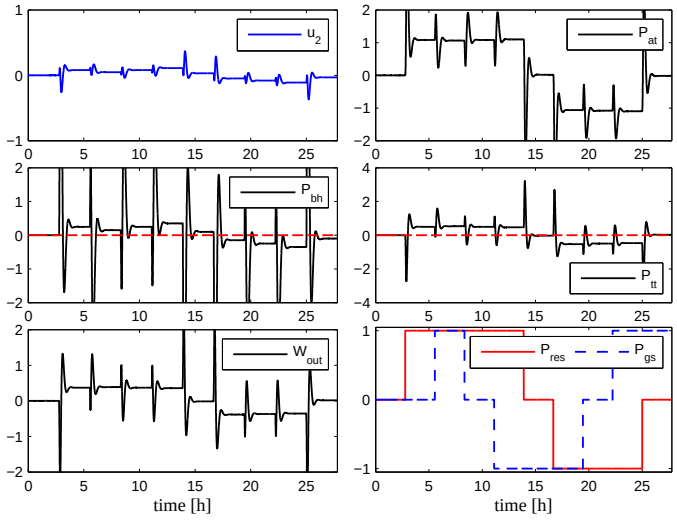

Fig. 10. Simulation result of $\mathcal{H}_\infty$ control using P_{bh} and P_{tt} as control variables and and u_2 as manipulated variable

Performance, robustness and input usage requirements were integrated in a mixed-sensitivity control problem and a single number (γ) was represented to evaluate quality of alternative control structures. We found out that adding the secondary manipulated variable does not improve stabilization of the gas-lifted oil wells significantly.

The bottom-hole pressure is the best control variable for this system in terms of controllability. Nevertheless, this variable often is not directly measurable.

Finally, a control structure using a pair of top-side pressure measurements was shown to be effective for preventing the casing-heading instability.

Further, it was found that accuracy of the sensors must be taken into account for scaling of different control variables correctly.

ACKNOWLEDGEMENTS

Financial support for this research was provided by Oil and Gas Division of SIEMENS.

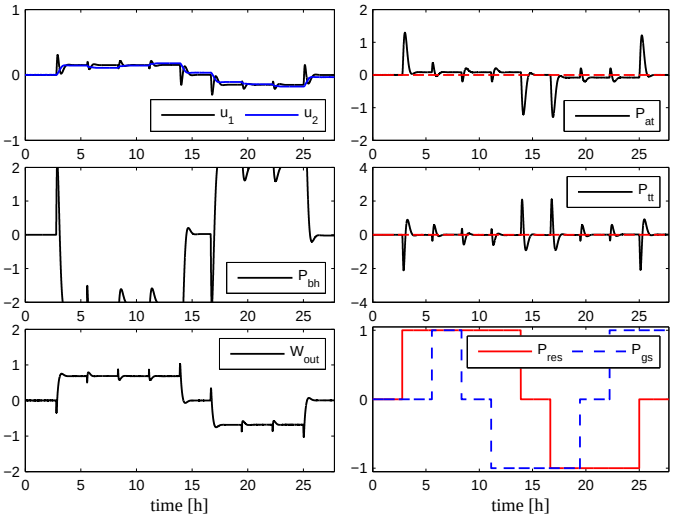

Fig. 11. Simulation result of $\mathcal{H}_\infty$ control for P_{at} and P_{tt} as control variables using MIMO controller

REFERENCES

Aamo, O., Eikrem, G., Siahaan, H., and Foss, B. (2005). Observer design for multiphase flow in vertical pipes with gas-lift - theory and experiments. *Journal of Process Control*, 15(3), 247 – 257.

Ahmed, T. (2006). *Reservoir Engineering Handbook, Third Edition*. Elsevier, Oxford, UK.

Dvergsnes, S. (1999). Modeling and control of gas-lifted oil wells. *Masters thesis. Department of Engineering Cybernetics, NTNU*.

Eikrem, G.O., Imsland, L., and Foss, B. (2004). Stabilization of gas lifted wells based on state estimation. In *IFAC International Symposium on Advanced Control of Chemical Processes*. Hong Kong, China.

Haaland, S.E. (1983). Simple and explicit formulas for the friction factor in turbulent pipe flow. *Journal of Fluids Engineering*, 105(1), 89–90. doi:10.1115/1.3240948.

Imsland, L. (2002). *Topics in Nonlinear Control - Output Feedback Stabilization and Control of Positive Systems*. Phd thesis, Norwegian University of Science and Technology.

Jahanshahi, E. and Skogestad, S. (2011). Simplified dynamical models for control of severe slugging in multiphase risers. In *18th IFAC World Congress*, 1634–1639. Milan, Italy.

Jansen, B., Dalsmo, M., Nøkleberg, L., Havre, K., Kristiansen, V., and Lemetayer, P. (1999). Automatic control of unstable gas lifted wells. In *SPE Annual Technical Conference and Exhibition*. Houston, Texas.

Sivertsen, H., Alstad, V., and Skogestad, S. (2009). Medium-scale experiments on stabilizing riser-slug flow. *SPE Projects, Facilities & Construction*, 4(4), 156–170, SPE no. 120040.

Skogestad, S. and Postlethwaite, I. (2005). *Multivariable Feedback Control: Analysis and Design*. Wiley & Sons, Chichester, West Sussex, UK.

Storkaas, E. and Skogestad, S. (2007). Controllability analysis of two-phase pipeline-riser systems at riser slugging conditions. *Control Engineering Practice*, 15(5), 567–581.